

Loss of *Tbx4* blocks hindlimb development and affects vascularization and fusion of the allantois

L. A. Naiche and Virginia E. Papaioannou*

Department of Genetics and Development, College of Physicians and Surgeons, Columbia University, 701 W. 168th Street, New York, NY 10032, USA

*Author for correspondence (e-mail: vep1@columbia.edu)

Accepted 14 March 2003

SUMMARY

Tbx4 is a member of the T-box family of transcription factor genes, which have been shown to play important roles in development. We have ablated *Tbx4* function using targeted mutagenesis in the mouse. Embryos homozygous for the null allele fail to undergo chorioallantoic fusion and die by 10.5 days post coitus. The allantoises of *Tbx4*-mutant embryos are stunted, apoptotic and display abnormal differentiation. Endothelial cells within mutant allantoises do not undergo vascular remodeling. Heterozygous embryos show a mild, transient growth defect in the allantois. Induction of a hindlimb field occurs normally in

Tbx4 mutants and initial patterning of the hindlimb bud appears normal. However, hindlimb buds from *Tbx4* mutants fail to develop either in vivo or in vitro and do not maintain *Fgf10* expression in the mesenchyme. The expression of another, closely-linked, T-box gene, *Tbx2*, is reduced in both the hindlimb and the allantois of *Tbx4*-mutant embryos prior to the development of overt morphological abnormalities, which suggests that *Tbx4* regulates *Tbx2* in these tissues.

Key words: *Tbx4*, T-box, Mouse, Allantois, Limb, Vasculogenesis

INTRODUCTION

T-box genes encode a family of transcription factors that contain a conserved DNA-binding motif known as the T-box domain (Papaioannou, 2001). Members of this family are expressed dynamically during development, and mutations in T-box genes have profound effects on development in organisms ranging from *C. elegans* to humans. In vertebrates, the *Tbx2* subfamily of T-box genes consists of four members, *Tbx2*, *Tbx3*, *Tbx4* and *Tbx5* (Ruvinsky et al., 2000), and in vertebrate species where all members have been cloned (mouse, chick and human) they are highly conserved. The *Tbx2* subfamily consists of two pairs of linked genes, which are thought to be the product of an ancestral tandem duplication, followed by duplication and dispersion of the two-gene clusters (Agulnik et al., 1996). The genes of one cluster, *Tbx3* and *Tbx5*, cause dominant developmental syndromes in humans, known as ulnar-mammary (Bamshad et al., 1997) and Holt-Oram (Basson et al., 1997; Li et al., 1997) syndromes, respectively. In mouse, mutations in *Tbx3* and *Tbx5* also cause developmental abnormalities (Bruneau et al., 2001; Davenport et al., 2003). No mutations in genes of the other cluster, *Tbx2* and *Tbx4*, have been reported.

The first expression of *Tbx4* in the mouse embryo is observed at 7.5 days post coitus (dpc) in the developing allantois. This expression is maintained through at least 9.5 dpc (Chapman et al., 1996). The allantois is an extra-embryonic, mesodermal structure that forms a connection between the

posterior embryo and the chorion early in development. This structure later develops into the umbilicus, and is crucial in mammals for nutrient, waste and gas exchange between mother and embryo. Molecular pathways involved in development of the allantois are not well characterized. However, several targeted mutations in mice have indicated that bone morphogenetic protein (BMP) signaling is crucial for allantois development. Embryos mutant for *Bmp4* lack an allantois (Lawson et al., 1999), and chimeric embryos lacking *Bmp4* specifically in the epiblast lineage form only a small allantois that fails to fuse to the chorion (Fujiwara et al., 2001). Although neither *Bmp5*- nor *Bmp7*-mutant mice have allantois defects, the allantois of embryos doubly homozygous for both mutations fails to undergo chorioallantoic fusion (Solloway and Robertson, 1999). *Bmp8b* mutants also have shortened allantoises, and a reduced number of primordial germ cells (Ying et al., 2000). Furthermore, mutations in the downstream effectors of BMP signaling, *Smad1* (*Madh1* – Mouse Genome Informatics) and *Smad5* (*Madh5* – Mouse Genome Informatics), produce aberrant allantois morphology, although not as severe as that of the BMP mutations (Chang et al., 1999; Lechleider et al., 2001; Tremblay et al., 2001).

Several genes involved in the process of chorioallantoic fusion have been identified. The adhesion molecule VCAM1, which is expressed in the distal tip of the allantois, and its receptor, $\alpha 4$ integrin, which is expressed in the chorion, are both required for successful chorioallantoic fusion (Gurtner et al., 1995; Kwee et al., 1995; Yang et al., 1995). Additionally,

several transcription factors that are required for proper chorioallantoic fusion have been identified by targeted mutagenesis, including the forkhead transcription factor *Foxf1* (Mahlapuu et al., 2001) and *Suppressor of Hairless* homolog *RBP-J* κ (*Rbpsuh* – Mouse Genome Informatics) (Oka et al., 1995). Connection(s) between these various signaling factors, adhesion molecules and transcription factors have not been elucidated and previously no role in this process has been identified for *Tbx4*.

During organogenesis, *Tbx4* is expressed in a variety of tissues, including the hindlimb, proctodeum, mandibular mesenchyme, lung mesenchyme, atrium of the heart and the body wall (Chapman et al., 1996). Hindlimb expression of *Tbx4* initiates at 9.5 dpc in the posterior flank region known as the hindlimb field, before the hindlimb bud is formed. *Tbx5*, another *Tbx2* subfamily member, mirrors this expression pattern with forelimb-specific expression starting at 8.5 dpc, when the forelimb field is specified in the anterior flank. This reciprocal expression of *Tbx4* and *Tbx5* in the hindlimb and forelimb, respectively, is maintained throughout development (Chapman et al., 1996; Gibson-Brown et al., 1996).

Previous work has suggested that *Tbx4* plays a role in determining hindlimb identity. Transplants of limb mesenchyme and induction of ectopic limbs in chick show correspondence between the proportions of *Tbx4* and *Tbx5* expression, and the degree of forelimb versus hindlimb fate, respectively (Gibson-Brown et al., 1998; Isaac et al., 1998; Ohuchi et al., 1998). Ectopic expression of *Tbx4* and *Tbx5* in developing chick limbs results in limb abnormalities that may represent limb identity transformations (Rodriguez-Esteban et al., 1999; Takeuchi et al., 1999). Supporting evidence is offered by experiments with the homeodomain protein *Ptx1* (*Pitx1* – Mouse Genome Informatics), which is expressed specifically in the hindlimb (Lanctot et al., 1997; Shang et al., 1997) and which has also been suggested to play a role in hindlimb specification. Targeted mutagenesis of *Ptx1* produces mice with shortened hindlimbs that have characteristics of forelimbs (Lanctot et al., 1999; Szeto et al., 1999), and ectopic expression of *Ptx1* in chick forelimbs leads to both the upregulation of *Tbx4*, and the induction of the hindlimb-specific Hox genes *Hoxc10* and *Hoxc11* (Logan and Tabin, 1999).

Interpretation of the gain-of-function experiments with *Tbx4*, *Tbx5* and *Ptx1* in chick is confounded by the presence of endogenous *Tbx4* and *Tbx5* in the experimental limbs, and by limb abnormalities induced by overexpression of *Tbx4* and *Tbx5*, even in their endogenous domains (Rodriguez-Esteban et al., 1999; Takeuchi et al., 1999). We have therefore used targeted mutagenesis to investigate the role of *Tbx4* in the development of the hindlimb and other regions of *Tbx4* expression, including the allantois.

MATERIALS AND METHODS

Generation of *Tbx4* mutations in mice

A targeting vector was created using a total of 7.3 kb of genomic DNA from a 129Sv/J phage library (Stratagene, catalog number 946309). A *HindIII/EcoRV* fragment containing exons 4 and 5 was subcloned, and a *loxP*-flanked PGK-*neo* PGK-*thymidine kinase* dual selection cassette was inserted into the first *SpeI* site of intron 5 (Fig. 1A), giving homology 3 kb upstream and 5.3 kb downstream, respectively.

Oligonucleotides containing a third *loxP* site, as well as *KpnI*, *NheI* and *XhoI* sites, were ligated into the *XhoI* site 1.5 kb 5' of the selection cassette, in intron 4. The β -actin *diphtheria toxin* gene (Maxwell et al., 1987) was inserted at the distal 5' end of the targeting cassette for negative selection against random integration. This targeting construct was linearized and electroporated into R1 ES cells (Nagy et al., 1993). G418 resistant colonies were screened by Southern hybridization for homologous recombination events, using both 5' and 3' genomic probes (Fig. 1B,C). Approximately two-thirds of the clones containing the targeted *neo-tk* cassette also contained the 5' *loxP* site.

Chimeras were generated by injection of targeted ES cells into C57BL/6J blastocysts. ES cell-derived progeny of the chimeras and subsequent generations were routinely genotyped by PCR using the primers (a) 5'-GAGGATGTTCCCCAGCTAC-3' and (b) 5'-CAGTCTGAGAGGGTCAGACTC-3' (Fig. 1A,D), which detect a 500 bp endogenous band and a 550 bp mutant band containing the insertion of the engineered *loxP* site. Mice heterozygous for the *Tbx4^{tm1.1Pa}* allele were then mated to mice carrying the *cre* transgene under control of the β -actin promoter (Lewandoski and Martin, 1997), to generate the *Tbx4^{tm1.1Pa}* allele by excision of the selection cassette and a 1.5 kb genomic region (Fig. 1A). Confirmation of the *cre*-mediated excision of all *loxP*-flanked sequences and genotyping of mice with the *Tbx4^{tm1.1Pa}* allele was performed with the primers (a) and (b) above, and (c) 5'-TCATCTAGGCTTCACAGCC-3', which produces a 250 bp band (Fig. 1A,D).

Collection of embryos

Both the *Tbx4^{tm1.1Pa}* and the *Tbx4^{tm1.1Pa}* alleles were maintained on mixed genetic backgrounds. Mice heterozygous for each allele were intercrossed to generate homozygous mutant embryos. Noon on the day of a mating plug was considered 0.5 dpc. Embryos were dissected in phosphate buffered saline (PBS) with 0.2% bovine albumin (fraction V). All embryos were scored for chorioallantoic fusion prior to yolk sac removal. Yolk sacs were taken for PCR genotyping and embryos were fixed in 4% paraformaldehyde in PBS at 4°C for two hours or overnight, then dehydrated in methanol and stored.

Embryos dissected at 8.0 dpc were scored for somite number and for the extent of allantois elongation into the yolk sac cavity. Because the overall embryo size is quite variable at this point in development, allantois elongation was measured as a proportion of the distance between the posterior end of the embryo and the edge of the chorionic plate. Allantoises were scored as: 'early' if they had covered two-thirds or less than this distance; 'late' if they had covered more than two-thirds of the distance or if they had entered the dome formed by the chorionic plate; or 'fused' if they had formed a connection to the chorion.

In situ hybridization and immunohistochemistry

Whole-mount in situ hybridization was performed according to previously described protocols (Wilkinson and Nieto, 1993). Immunohistochemistry was performed according to standard protocols (Davis, 1993), except for VCAM1 immunohistochemistry, where DMSO was omitted from the bleach, PBSMT washes were replaced with PBSBT (4% BSA, 0.1% Triton X-100 in PBS) and primary antibody was diluted 1:150. Embryos used for doubly phosphorylated ERK protein (dp-ERK; EPHB2 – Mouse Genome Informatics) immunostaining were cut through the limb buds prior to bleaching to facilitate antibody penetration. Primary antibodies used included: anti-VCAM1 (PharMingen, catalog number 553330), anti-phospho-Histone H3 (Upstate Biotechnology, catalog number 06570), anti-PECAM (PharMingen, catalog number 01951D) and anti-phospho-p44/42 (anti-dp-ERK; Cell Signaling, catalog number 9101). All secondary antibodies were peroxidase-conjugated goat IgG from Jackson Immunochemicals.

PGC detection

Embryos were dissected at 8.0 dpc, scored as above and genotyped.

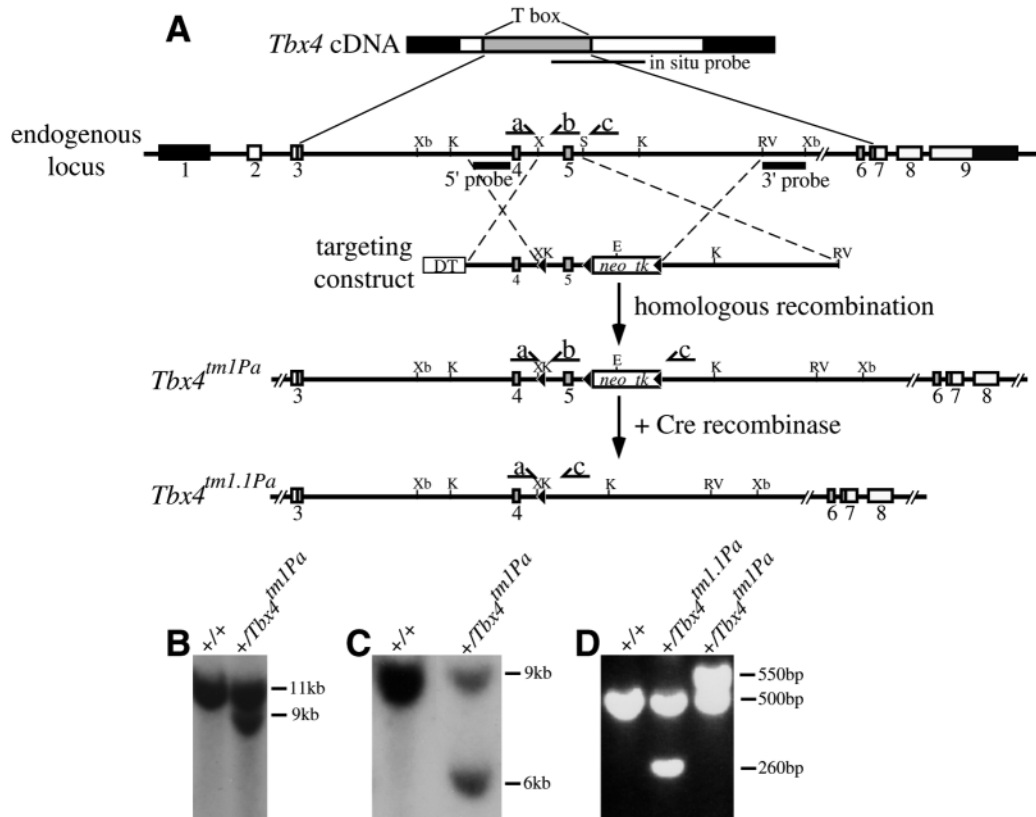


Fig. 1. Disruption of the *Tbx4* gene by homologous recombination in ES cells. (A) 7.3 kb of mouse genomic DNA was used to create a targeting construct containing a *loxP* site inserted into intron 4, a floxed PGK-*neo* PGK-*thymidine kinase* dual selection cassette (*neo tk*) inserted into intron 5 and a diphtheria toxin (DT) gene 5' of the homologous DNA for negative selection against random integration. The indicated region of the *Tbx4* cDNA was used for in situ hybridization (in situ probe). E, *EagI*; X, *XhoI*; Xb, *XbaI*; K, *KpnI*; S, *SpeI*; RV, *EcoRV*. Solid arrowheads indicate *loxP* sites. Boxes indicate exons: black, untranslated regions; white, coding regions; gray, T-box domain. Labeled boxes indicate selection cassettes. Figure not drawn to scale. (B) After electroporation, G418-resistant colonies were screened for homologous recombination by Southern hybridization of *EagI/XbaI* genomic digests probed with the 3' external probe shown in A. (C) Homologous recombination of the 5' end of the vector, including the *loxP* site, was confirmed using a *KpnI* digest probed with the 5' internal probe shown in A. (D) Oligonucleotides a and b were used to amplify the indicated genomic region by PCR, producing a 500 bp endogenous band and a slightly larger *Tbx4*^{tm1.1Pa} band with the *loxP* site insertion. Recombination of the *Tbx4*^{tm1.1Pa} allele was achieved by mating to a *cre*-expressing mouse. The recombined *Tbx4*^{tm1.1Pa} allele was genotyped using oligonucleotides a, b and c, to produce the same 500 bp endogenous band and a 260 bp mutant band.

Posterior halves were fixed in 4% paraformaldehyde in PBS for 1 hour at 4°C, and dehydrated in 70% ethanol for 3-6 hours. Embryos were rehydrated in NTMT, then stained with NBT/BCIP color reaction for 3 minutes (Wilkinson and Nieto, 1993) and photographed.

TUNEL assay

Terminal deoxynucleotidyl transferase biotin-dUTP nick end labeling (TUNEL) staining was performed using a Cell Death Detection kit (Roche, catalog number 1684817). Embryos were incubated in 10 µg/ml proteinase K for 8-10 minutes depending on stage, and refixed in 4% paraformaldehyde, 0.1% glutaraldehyde for 20 minutes at room temperature. Embryos were then incubated in TUNEL reaction mixture at 37°C for 1 hour, blocked with 10% sheep serum in PBT for 1 hour and incubated with the converter-POD mix (same kit) for 30 minutes at 37°C. Chromogenic reaction was developed with 0.08% NiCl₂ and 250 µg/ml diaminobenzidine in PBT for approximately 30 seconds.

Histology

At 8.25 dpc and 9.5 dpc, where simultaneous histology and genotyping were not possible, embryos were classified as mutant or

normal based on the appearance and fusion of the allantois. Three embryos were discarded from the analysis because they were grossly retarded compared to littermates. Embryos at 8.25 dpc and 9.5 dpc were removed intact in the uterine horns and fixed in Bouin's fix overnight. Embryos at 10.5 dpc were dissected out of the decidua, and the yolk sacs removed for genotyping before being similarly fixed. After dehydration in ethanol, embryos were embedded in paraffin wax, sectioned at 8 µm thickness and stained with Hematoxylin and Eosin.

Limb bud culture

Limb buds were dissected at 10.5 dpc in DMEM supplemented with 10 mM HEPES and 5% FCS. Explants were taken from embryos only if the embryo was alive and had a robustly beating heart. The embryo was transected immediately rostral and caudal to each set of limb buds (see Fig. 4A,F). Tissue ventral of the limb buds, including the heart and allantois, was trimmed off and the explant was placed ventral side down on a Transwell Clear (Costar) membrane. Explants were cultured for 4-7 days in DMEM/F-12 (Gibco BRL) with 10% FCS (Hyclone), 5× MITO⁺ Serum Extender (Becton Dickinson, catalog number 355006) at 37°C in 5% CO₂ in air.

RESULTS

Generation and inheritance of *Tbx4*-mutant alleles

The *Tbx4* gene was disrupted by the insertion, via homologous recombination in ES cells, of a *loxP* site and a *loxP*-flanked *neomycin-thymidine kinase* selection cassette into the introns surrounding exon 5 (Fig. 1A, *Tbx4^{tm1Pa}* allele). Correctly targeted ES cells were identified by Southern blotting (Fig. 1B,C). Targeted ES cells were injected into C57BL/6J blastocysts to create chimeras, which were mated to identify germline transmission of the mutant allele *Tbx4^{tm1Pa}*. Transmission of two ES cell lines of the *Tbx4^{tm1Pa}* allele produced by independent targeting events was obtained. Mice derived from both cell lines have the same phenotype and the results have been combined in this report. Mice heterozygous for the *Tbx4^{tm1Pa}* allele were mated to mice ubiquitously expressing a β -actin-*cre* transgene (Lewandoski and Martin, 1997) to excise both the selection cassette and the floxed exon 5, thereby creating the *Tbx4^{tm1.1Pa}* allele (Fig. 1A).

Heterozygous mice of both alleles were apparently normal and fertile. Heterozygotes were intercrossed to generate embryos homozygous for each allele. Both the *Tbx4^{tm1Pa}* allele and the Cre-recombined *Tbx4^{tm1.1Pa}* allele were inherited in Mendelian ratios, but all homozygous mutants dissected after 10.5 dpc were dead (Table 1). In litters that were allowed to go to term, no homozygous mutants were observed among weanlings ($n=397$ and $n=108$, for the *Tbx4^{tm1Pa}* and *Tbx4^{tm1.1Pa}* alleles, respectively). All analyses, including in situ hybridizations for limb marker genes, were performed on embryos homozygous for each allele. Results for each were the same, and so have been combined in this report.

Development and morphological defects of *Tbx4*-homozygous mutants

Tbx4-homozygous-mutant embryos display no apparent morphological abnormality until 8.0 dpc, when an allantois defect becomes evident. At this age, normal embryos have well-formed allantoises that elongate from the posterior end of the embryo and fuse with the chorionic plate at the 6- to 8-somite stage (Fig. 2A). *Tbx4*-mutant embryos of the same age display allantoises extended only partway through the yolk sac cavity, and 6- to 8-somite stage mutant embryos have not undergone chorioallantoic fusion (Fig. 2B). Homozygous-mutant embryos turn at the same stage as their normal littermates. By 9.5 dpc, normal embryos have formed a thick,

vascular umbilicus (Fig. 2C) connecting the embryo to the placenta, whereas mutant embryos remain loose in the yolk sac, unattached to the placenta (Fig. 2C). No other abnormalities were seen at 9.5 dpc.

At 10.5 dpc, *Tbx4*-mutant embryos are loose in the yolk sac: some display swollen pericardial sacs and/or hemorrhage (Fig. 2D), and many are dead, as judged by the absence of a heartbeat. All homozygous mutants dissected after 10.5 dpc were dead (Table 1). Instead of the umbilical vessels of the wild type (Fig. 2E), the allantois of 10.5 dpc mutant embryos forms a compact amorphous mass surrounding blood-filled vesicles (Fig. 2F). There is no obvious leakage of blood from the residual allantois into the yolk sac cavity. At the latest stage reached by the homozygous mutants prior to their death (~29-32 somites), mutant embryos have morphologically apparent hindlimb buds (Fig. 2D). Hindlimb buds in 27- to 29-somite mutant embryos are similar in size to somite-matched normal littermates, but are modestly reduced in size in 30- to 32-somite mutant embryos when compared with somite-matched controls.

Two 10.5 dpc *Tbx4*-mutant embryos (representing less than 1%) have been observed in which the developing allantois had made a connection with the chorion. In both embryos the allantois was small and irregular, consisting of multiple blood-filled chambers. In each case, the allantoic attachment to the chorion was at only a single point, and had not spread over the chorionic surface. No apparent continuous vessel had formed between the embryo and the placenta, and no flow of blood could be detected.

Histological examination of *Tbx4*-mutant embryos

Histological examination of 8.25 dpc embryos revealed multiple abnormalities in the allantois of *Tbx4*-mutant embryos. The wild-type allantois at this stage ($n=10$) is a funnel shaped structure tightly opposed to the chorion at the wide end and tapering towards the posterior end of the embryo (Fig. 2G). The mesenchyme near the embryo is dense and uniform, whereas near the chorion it is loose and cavitated. In mutant embryos ($n=2$), the allantois was not opposed to the chorionic plate and there was no evidence of allantois-derived cells adherent to the chorion (Fig. 2H), although the chorion itself appeared normal. The mutant allantois shows dense, irregularly packed cells in the base of the allantois, with multiple double-walled vesicles (Fig. 2I) and numerous pyknotic nuclei, which is indicative of dying cells.

Table 1. Genotypes of embryos from *Tbx4* heterozygous intercrosses at different embryonic ages

Allele	Genotype	Age (dpc)								Total [§]
		8.0	8.5	9.0	9.5	10.5	11.0	11.5	13.5	
<i>Tbx4^{tm1Pa}</i>	+/+	56	29	5	7	87	6	1	0	191
	+/-	127	45	13	20	176	8	5	5	399
	-/-	60	18	7	9	84*	5 [‡]	3 [‡]	2 [‡]	188
<i>Tbx4^{tm1.1Pa}</i>	+/+	8	1	nd	8	36	nd	0	nd	53
	+/-	15	5	nd	15	88	nd	3	nd	126
	-/-	14	4	nd	7	48 [†]	nd	3 [‡]	nd	76

*Approximately 20% of -/- embryos dissected before 1.00 pm were dead. 53% of -/- embryos dissected after 1.00 pm were dead.

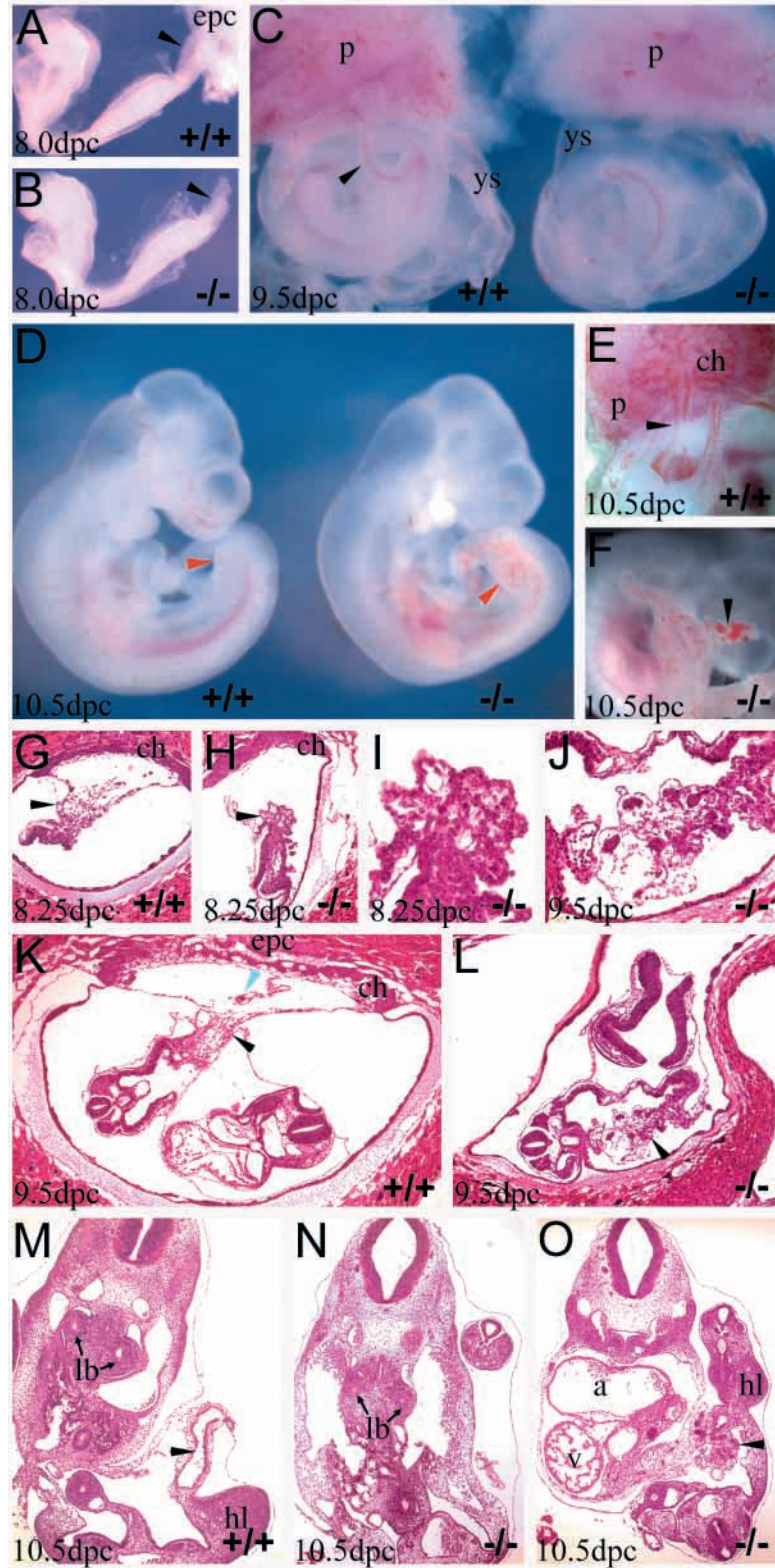
[†]Approximately 20% of -/- embryos dissected before 1.00 pm were dead.

[‡]Embryos were dead and degenerating. Genotypes were obtained from the yolk sac or the embryonic part of the placenta.

[§]No significant differences from Mendelian ratios of inheritance were found for *Tbx4^{tm1Pa}* ($\chi^2=0.54$, $P>0.25$) and *Tbx4^{tm1.1Pa}* ($\chi^2=4.18$, $P>0.15$). nd, not done.

At 9.5 dpc, the allantois of wild-type embryos ($n=4$) consists of moderately dense mesenchyme with a more open structure near the chorion. Blood vessels running through the allantois are visible (Fig. 2K). By contrast, the allantois of a mutant at this stage ($n=1$) was small and dense, and had numerous condensed cells (Fig. 2J,L). At 10.5 dpc, sections through a

wild-type embryo show a developing hindlimb bud and an umbilical vessel (Fig. 2M). Sections through a *Tbx4* mutant embryo show some edema, but an otherwise normal development in embryonic tissues, including lung buds, heart, fore- and hindlimb (Fig. 2N,O). However, the allantois at this stage has not developed further, and consists of irregular mesenchyme with multiple irregularly shaped, dense condensations of cells and occasional empty vesicles (Fig. 2O).



Growth and cell proliferation in *Tbx4*-mutant allantoises

Embryos dissected at 8.0 dpc were scored for allantois phenotype and somite number (Fig. 3A). Differences between wild-type and mutant embryos become apparent as early as the 4- to 5-somite stage, when wild-type embryos are mostly at the late allantois stage or fused to the chorionic plate but most *Tbx4*-mutants are still at the early bud stage.

Fig. 2. Morphology of wild-type (+/+) and *Tbx4*-homozygous mutants (-/-). Black arrowhead indicates the allantois or umbilicus. (A) An 8-somite wild-type embryo. The allantois has fused with the chorion and ectoplacental cone (epc). (B) An 8-somite *Tbx4*-mutant embryo shows a stunted, unfused allantois. (C) 9.5 dpc embryos partially dissected out of the yolk sac (ys). The allantois of the wild-type embryo has formed a vascular umbilicus connecting it to the placenta (p), whereas the mutant embryo is loose in the yolk sac and the allantois has formed only a small, amorphous stump. (D) 10.5 dpc wild-type and mutant embryos dissected out of their membranes. The mutant is hemorrhagic and has only the stump of an allantois, but it is otherwise normal and shows a distinct hindlimb bud similar to that of the wild type (red arrowheads). (E) Close-up of a wild-type umbilical connection at 10.5 dpc, with large umbilical blood vessels connected to the chorionic plate (ch) of the placenta. (F) Close-up of the unfused allantoic stump of a *Tbx4* mutant at the same stage, which is not connected to the placenta and shows no coherent blood vessels. (G) Section through a normal 8.25 dpc allantois. The allantois has a funnel shape, the chorionic end of which contains loose, cavitated mesenchyme and a layer of cells tightly opposed to the chorion; the base has a more compact, uniform mesenchyme. (H) Section through the base of an unfused mutant allantois, showing dense cell packing and distinctive vesicles. (I) Detail of H, showing two of the characteristic mutant double-layered vesicles and cell debris from dying cells. (J) Detail of L, showing the mutant allantois at 9.5 dpc. The irregular mesenchyme contains dense condensations that have no apparent connections between them in serial sections. (K) Section through a normal 9.5 dpc allantois and embryo. Blue arrowhead indicates a blood vessel in the allantois. (L) Section through a mutant 9.5 dpc allantois and embryo. The allantois is unfused and the chorion is out of the section plane at the top. Embryonic tissues appear normal. (M) Transverse section through a wild-type 10.5 dpc embryo, with normal lung buds (lb), hindlimb bud (hl) and umbilicus. (N) Transverse section of a 10.5 dpc mutant in a similar plane as the embryo in M, as indicated by the lung buds. All structures appear normal. (O) A more ventral section of the same embryo showing a normal heart (a, atrium; v, ventricle), a small hindlimb bud (hl) and the remnants of an allantois.

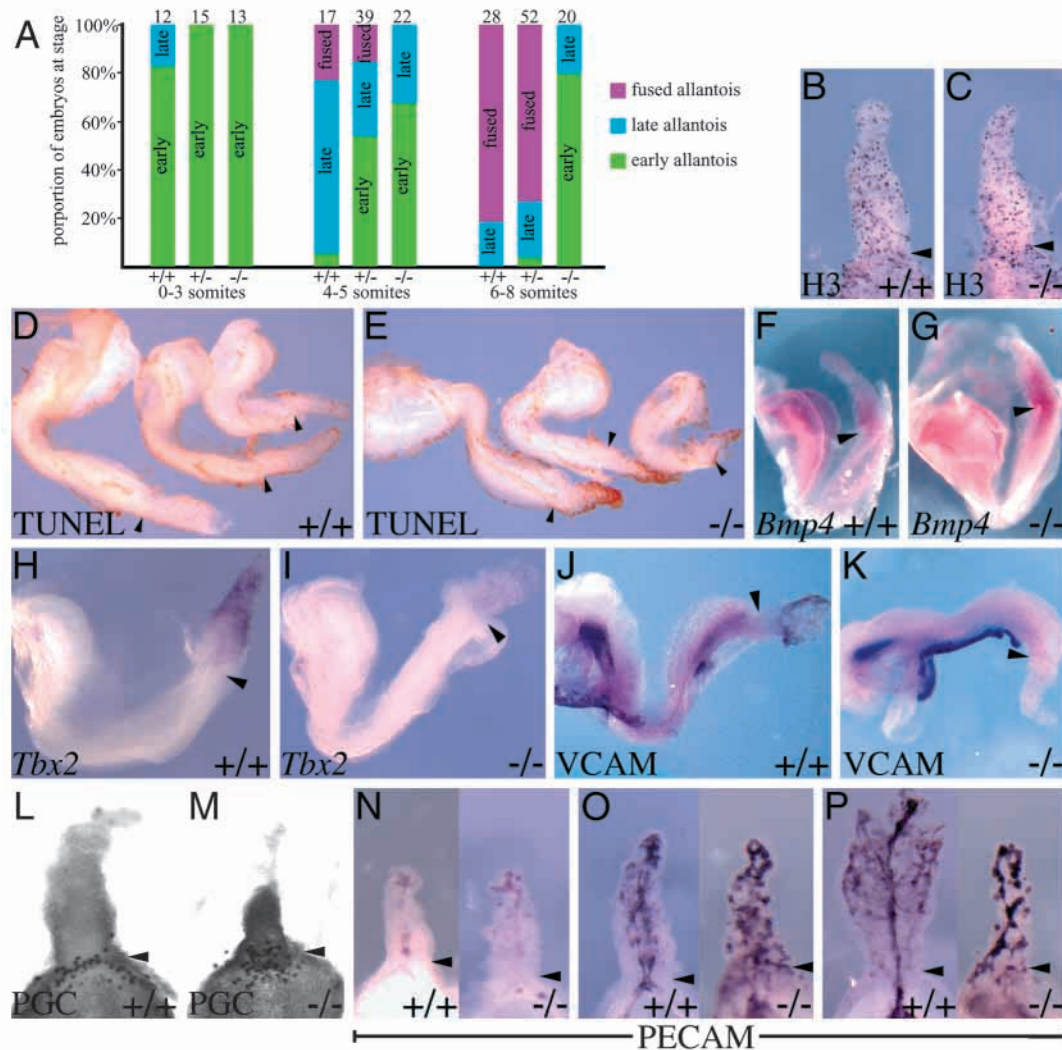


Fig. 3. Growth and differentiation of wild-type (+/+) and *Tbx4*-mutant (-/-) allantoises. All embryos were dissected at 8.0 dpc and were at the 0- to 8-somite stages. Black arrowheads indicate the base of the allantois in all panels. (A) A summary of 8.0 dpc embryos grouped by somite number and genotype and scored for extension of the allantois as early, late or fused (see methods). Each section of the stacked bar represents the proportion of those embryos at a specific allantois stage. The number in each set is shown at the top of the bar. (B,C) Anti-phospho-Histone H3 staining showing cells undergoing mitosis. The wild-type (B) and the mutant (C) allantoises show similar numbers of mitotic cells, both in the base of the allantois and in the distal tip. (D,E) Sets of 0- to 8-somite embryos (somite number decreases to the right in each panel) TUNEL stained to indicate apoptotic cells. Although wild-type embryos (D) show few apoptotic cells, the mutant embryos (E) exhibit extensive cell death over the entire distal portion of the allantois. (F,G) *Bmp4* is expressed in the base of the allantois in wild-type (F) and mutant (G) embryos. (H,I) *Tbx2* is expressed in the distal two-thirds of the wild-type allantois at the 2-somite stage (H), but is extremely faint in mutant allantoises (I). (J,K) The cell adhesion molecule VCAM1 is expressed in the distal tip of the allantois in wild-type (J), but not mutant (K), embryos. (L,M) Endogenous alkaline phosphatase staining marks the PGCs, which are similar in location and number in wild-type (L) and mutant (M) embryos. (N-P) PECAM marks differentiating endothelial cells, which in the wild type appear in clumps at the 0-somite stage (N); they elongate into small vessels at the 4-somite stage (O) and resolve into a central vessel at the 8-somite stage (P). In *Tbx4* mutants (N-P), normal looking clumps appear at 0 somites, whereas at 4 somites more clumps have appeared but no elongated vessels are seen. At the 8-somite stage, no central vessel is seen.

Heterozygous embryos at the 4- to 5-somite stage exhibit a lag in allantois development when compared with somite-matched wild-type controls. At the 6- to 8-somite stage, nearly all wild-type and heterozygous embryos have undergone chorioallantoic fusion, whereas most mutant embryos are at the early allantois stage. All wild-type and heterozygous embryos past the 8-somite stage have completed chorioallantoic fusion.

To further investigate the allantois growth defect, we

examined the rate of cell proliferation and cell death in this tissue. Cellular proliferation in mutant allantoises (Fig. 3C) is comparable to wild-type embryos of the same stage (Fig. 3B), and mitotic cells are seen at all levels of the allantois, including the distal tip. TUNEL staining shows little or no apoptotic cell death in the allantois of wild-type embryos (Fig. 3D), whereas homozygous-mutant embryos exhibited extensive cell death over the entire distal tip of the allantois (Fig. 3E).

Abnormal differentiation within the allantois in *Tbx4* mutants

The differentiative capacity of the allantois in the absence of *Tbx4* was assessed by examining the expression of a number of genes with characteristic expression patterns during normal allantois development. *Bmp4* expression, which is required for proper allantois development, is apparent in the base of both wild-type (Fig. 3F) and mutant (Fig. 3G) allantoises. *Tbx2* is expressed in the wild-type allantois (Fig. 3H) from its earliest morphological appearance until early 9.5 dpc (Chang et al., 1999; Mahlapuu et al., 2001) (L.A.N. and V.E.P., unpublished). In *Tbx4*-homozygous mutants, *Tbx2* expression is absent or dramatically reduced in the allantois of the 2-somite embryo (Fig. 3I), and entirely absent in the allantois of later embryos (data not shown).

Contrary to previous work published by this lab (Chapman et al., 1996), we were unable to detect *Tbx5* expression in the allantois by whole-mount in situ hybridization. No *Tbx5* expression was seen in the allantois of either mutant or wild-type embryos from 7.5 dpc to 8.5 dpc, although expression in the heart crescent was visible from late 7.5 dpc onward as expected (data not shown). The brachyury gene (*T*), which marks the primitive streak, notochord and the base of the allantois, is expressed normally in the *Tbx4*-mutant allantoises (data not shown). VCAM1, a cell adhesion molecule required for allantoic fusion, is seen by antibody staining in the extreme distal end of the fused allantois in the 8-somite wild-type embryo (Fig. 3J), but is absent from the unfused distal tip of *Tbx4*-mutant allantoises (Fig. 3K).

The primordial germ cells (PGCs) form a group of alkaline phosphatase-positive cells at the base of the allantois at 8.0 dpc, shortly before they migrate along the dorsal mesentery to the future gonads. Their formation is impaired in some of the BMP pathway mutations that affect allantois development (Lawson et al., 1999; Tremblay et al., 2001; Ying et al., 2000). In wild-type (Fig. 3L) and *Tbx4*-mutant (Fig. 3M) embryos, PGCs appear to be similar in number and location.

To assess vascularization in the allantois, we examined the appearance of PECAM-1 (PECAM – Mouse Genome Informatics), a late marker of endothelial cell development. In wild-type embryos at the 0- to 2-somite stage, anti-PECAM-1 antibody marks small clumps of endothelial cells in the allantois (Fig. 3N). At the 3- to 4-somite stage, these PECAM-positive cells form multiple small vessels (Fig. 3O). By the 6- to 8-somite stage, these vessels have largely collected into a central vessel(s) at the base of the allantois, with unincorporated vessels still apparent distally (Fig. 3P). In *Tbx4* mutants, expression of PECAM-1 initiates normally (Fig. 3L), but soon acquires a strikingly different appearance. Numerous small clumps of PECAM-positive cells appear along the length of the allantois, but these fail to elongate into vessels and no central vessel is formed (Fig. 3O,P).

In vitro culture of *Tbx4*-mutant hindlimbs

To investigate the role of *Tbx4* in hindlimb development beyond the time of death of *Tbx4*-mutant embryos, limb buds from 10.5 dpc embryos were grown in culture. Both forelimb and hindlimb buds were dissected from live 10.5

dpc mutant embryos and littermate controls, and explanted onto membranes suspended on growth media (Fig. 4B,C,G,H) to examine their developmental potential. After 3 days of growth, forelimb buds of both normal (Fig. 4D) and homozygous *Tbx4*-mutant embryos (Fig. 4E) exhibited an increase in the distance between the right and left distal limb margins, corresponding to outgrowth of the limbs from the midline. Cultured limb buds also assumed the paddle-shaped

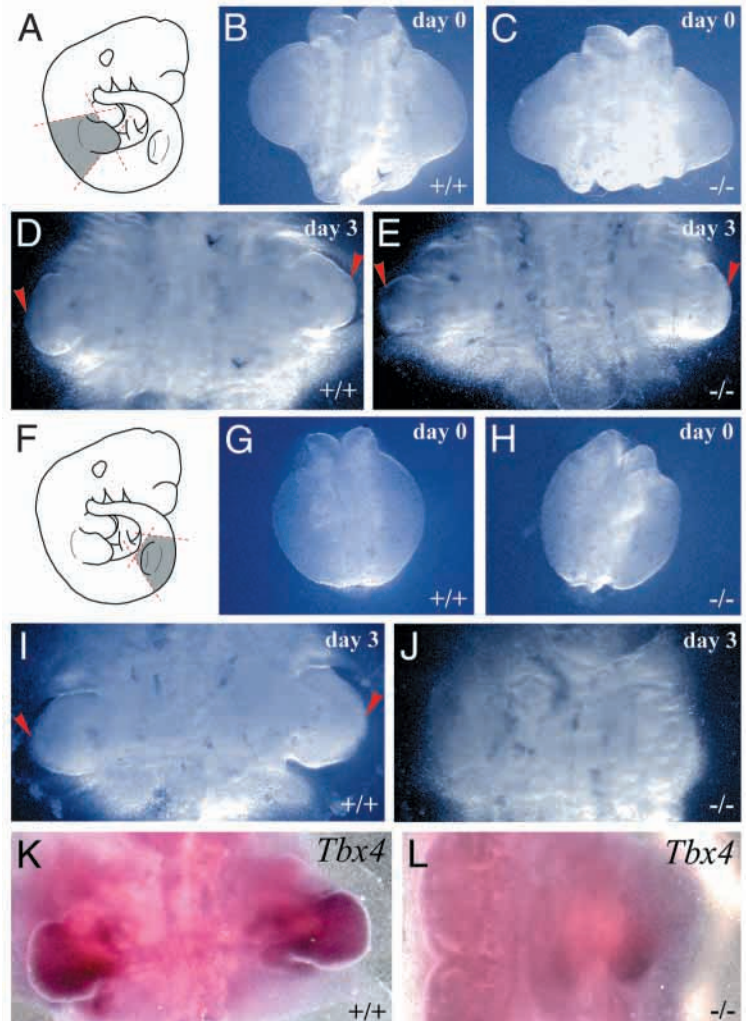


Fig. 4. In vitro culture of forelimb and hindlimb buds from 10.5 dpc embryos. (A) Forelimb tissue explanted at 10.5 dpc. Dashed lines indicate planes of dissection; gray area represents tissue explanted. (B,C) Forelimb buds dissected from normal and mutant embryos, respectively, immediately after explantation. (D,E) Forelimb explants from control and mutant embryos, respectively, show an increase in distance between the distal limb margins (arrowheads) and the development of a paddle-shaped autopod after 3 days in culture. (F) Explanted hindlimb tissue. (G,H) Hindlimb buds from normal and mutant embryos, respectively, immediately after dissection. (I) Control hindlimb buds also exhibit increased distance between limb margins (arrowheads) and autopod development after 3 days in culture. (J) By contrast, explants from *Tbx4*-mutant embryos have no visible limb structures remaining after the same time period. (K,L) Limb explants hybridized with a *Tbx4* probe from outside the region deleted in the mutant. The wild type (K) expresses *Tbx4* in the morphologically apparent hindlimb buds, whereas the mutant explant (L) shows only faint *Tbx4* expression, and regions of *Tbx4* expression show no morphological limb structure. All panels are at the same magnification.

morphology of handplate stage limbs. After the same culture period, wild-type hindlimb buds had also expanded distally and developed a recognizable paddle-shaped handplate (Fig. 4I, $n=23$), but mutant hindlimb explants failed to develop any obvious limb structures (Fig. 4J, $n=11$). To verify the identity of these limb structures, *in situ* hybridizations were performed on cultured explants using a *Tbx4* probe from outside of the deleted region as a hindlimb marker (Fig. 1A). The mutant transcript was expressed normally in homozygous mutants at all stages examined. *Tbx4* was clearly expressed in the handplate paddles of wild-type embryos (Fig. 4K), but it was expressed only in a few scattered patches of cells, with no obvious limb morphology, in mutant embryos (Fig. 4L).

Hindlimb bud initiation in *Tbx4* mutants

To explain the absence of growth of the *Tbx4*-mutant hindlimbs in culture despite the presence of a morphologically obvious hindlimb bud, we examined the expression of genes known to be involved in the initiation and maintenance of limb formation (Martin, 2001) prior to the development of the mutant phenotype. Limb outgrowth is known to be maintained by a mesenchymal-ectodermal feedback loop. Mesenchyme from the limb field signals to the overlying ectoderm through *Fgf10* to induce the apical ectodermal ridge (AER). Limb ectoderm then signals back to the mesenchyme through several molecules, including FGFs. This reciprocal signaling is necessary for the maintenance of many limb mesenchyme genes, including *Fgf10*.

Fgf8 is an early marker of the AER, and is expressed normally in a narrow strip along the dorsoventral margin of both wild-type and *Tbx4*-mutant hindlimb buds (Fig. 5A,B), indicating that successful initial induction of the AER has occurred. *Msx1*, which lies downstream of limb ectodermal signaling (Wang and Sassoon, 1995), is also expressed normally in *Tbx4*-mutant hindlimbs (Fig. 5C,D). The twist gene, which is required in limb mesenchyme for the FGF-mediated feedback loop and for proper FGF receptor expression in the limb mesenchyme (O'Rourke et al., 2002; Zuniga et al., 2002), is also expressed normally in *Tbx4* mutants (Fig. 5E,F).

To confirm that *Tbx4*-mutant limb mesenchyme receives FGF signals from the ectoderm, we examined the distribution of doubly phosphorylated ERK protein (dp-ERK), which is present when activated FGF receptors activate the mitogen-activated kinase (MAPK) cascade. At this very early stage of limb induction, dp-ERK staining is found asymmetrically in the hindlimbs with staining first appearing in the right hindlimb (Fig. 5G), although it evens out in more developmentally advanced limbs (data not shown). dp-ERK is observed in *Tbx4*-mutant hindlimb buds in the same asymmetric pattern, demonstrating mesenchymal reception of ectodermal FGF signals (Fig. 5G,H). However, despite an apparently normal limb induction and normal FGF-feedback signaling, *Fgf10* is not maintained in *Tbx4*-hindlimb mesenchyme and is only seen in the flank underlying the hindlimb bud (Fig. 5I,J). As *Fgf10* is required for limb outgrowth, this defect could explain the absence of *Tbx4*-mutant hindlimb development *in vitro*.

Hindlimb patterning in *Tbx4* mutants

As *Tbx4* expression is specific to the hindlimb and has been postulated to have a role in specifying hindlimb identity, we

examined other genes that have differential expression between fore- and hindlimbs. The domain of *Tbx5*, which is normally expressed specifically in the forelimb, is unaltered in *Tbx4*-mutant embryos (Fig. 6A,B), indicating that *Tbx4* plays no role

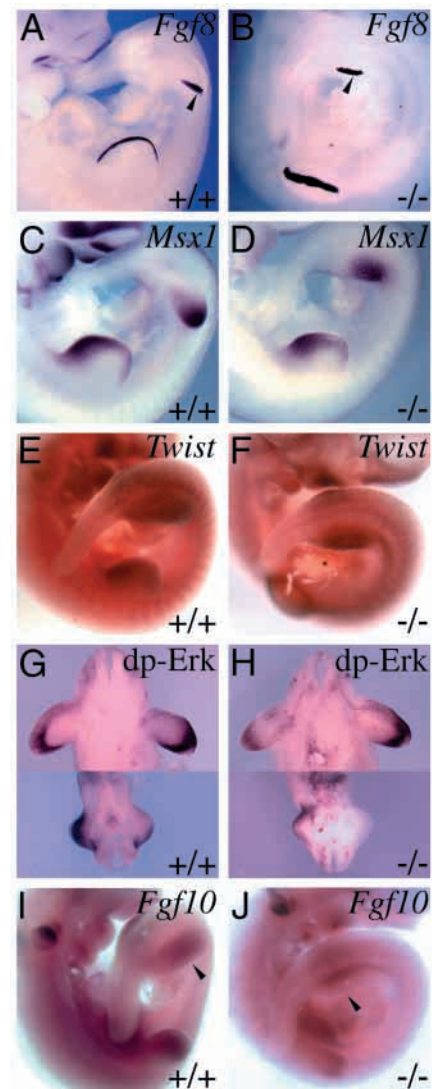


Fig. 5. Expression of genes involved in limb bud initiation in wild type (+/+) and *Tbx4* mutants (-/-) at 10.5 dpc. (A,B) *Fgf8* expression is visible in the AER of the forelimb bud and the presumptive AER of the hindlimb bud in wild-type and *Tbx4*-mutant embryos. (C,D) Expression of *Msx1* is present in the mesenchyme of the forelimbs and hindlimbs of both wild-type and mutant embryos. (E,F) *Twist* is expressed normally throughout the hindlimb mesenchyme of wild-type and mutant embryos. (G,H) Thick sections through the forelimbs (top) and hindlimbs (bottom) of 10.5 dpc embryos. Anti-dp-ERK marks regions of FGF signaling and is seen in the mesenchyme immediately underlying the AER of forelimbs, and asymmetrically in the mesenchyme of the hindlimbs in the wild-type embryo. *Tbx4*-mutant embryos also show similar dp-ERK staining in both sets of limbs. (I,J) *Fgf10* is expressed in the distal mesenchyme of the forelimb and throughout the mesenchyme of the hindlimb bud of the wild type. In *Tbx4* mutants, forelimb expression of *Fgf10* is unaltered, but expression in the hindlimb appears only in the proximal mesenchyme and is absent from the distal hindlimb bud. Arrowheads indicate the distal edge of hindlimb bud.

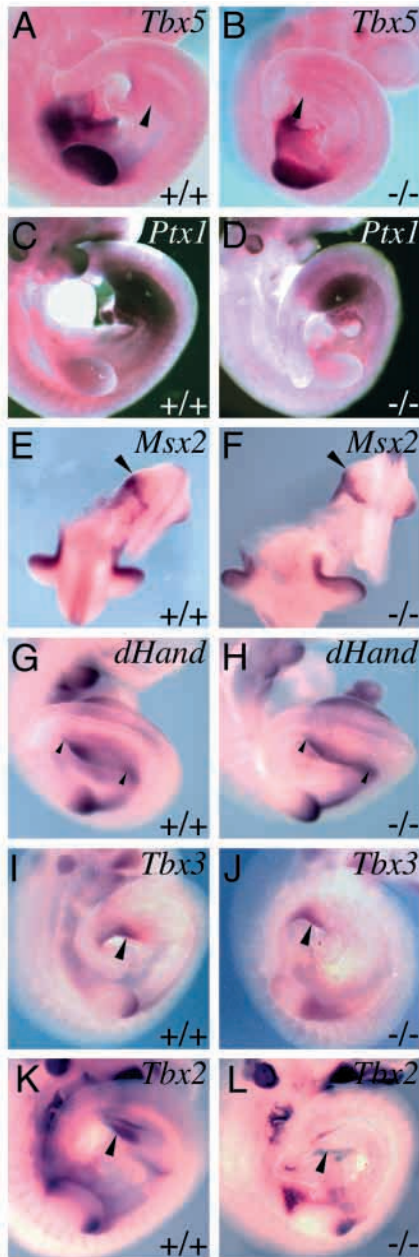


Fig. 6. Expression of limb patterning genes in the limb buds of wild-type (+/+) and *Tbx4*-mutant embryos (-/-) at 10.5 dpc. (A,B) *Tbx5* is expressed in the forelimb bud and absent in the hindlimb bud (arrowheads) of wild-type and mutant embryos. (C,D) *Ptx1* is expressed in the hindlimb bud, but not the forelimb bud of both wild-type and mutant embryos. (E,F) *Msx2* marks the ventral limb ectoderm in both normal and mutant hindlimb buds. Embryos are oriented for a posterior view of the hindlimb bud, with forelimbs at the bottom of the picture and the head removed for clarity. Arrowheads mark the dorsal boundary of *Msx2* expression in the hindlimb. (G,H) *dHand*, an upstream regulator of *Shh*, is expressed strictly in the posterior edge of the hindlimb bud of normal embryos, but throughout the margin of the *Tbx4*-mutant hindlimb bud. Small arrowheads mark anterior and posterior boundaries of the hindlimb bud. (I,J) *Tbx3* is expressed in the posterior edge of both forelimb and hindlimb buds (arrowheads) in both wild-type and mutant embryos. (K) *Tbx2* is expressed in both anterior and posterior edges of the forelimb bud and in the posterior edge of the wild-type hindlimb bud (arrowhead). (L) In the *Tbx4* mutants, *Tbx2* is normally expressed in the forelimb but absent from the posterior hindlimb.

in maintaining this differential expression. Likewise, the *Tbx4*-expression domain (visualized with a probe from outside of the deleted region) in the hindlimb is retained in *Tbx4* mutants (data not shown). *Ptx1*, which is co-expressed in the hindlimb field with *Tbx4*, is also unaltered in the *Tbx4*-mutant hindlimb field (Fig. 6C,D). Unfortunately the death of *Tbx4*-mutant embryos in vivo, and the absence of hindlimb growth in vitro, preclude the study of later fore- and hindlimb specific genes, such as limb-specific Hoxc genes.

We also examined early markers of dorsoventral and anterior/posterior axis formation in the hindlimb. *Msx2*, which marks the ventral limb ectoderm, is expressed ventrally in *Tbx4*-mutant hindlimb buds (Fig. 6E,F). We were unable to observe the expression of *Shh*, the definitive marker of the posterior zone of polarizing activity (ZPA) function, as this gene is not expressed in the hindlimb until late 10.5 dpc, after *Tbx4* mutants are dead (data not shown). However, we did examine *dHand* (*Hand2* – Mouse Genome Informatics), which lies upstream of *Shh* and is also normally restricted to the posterior edge of limb buds. In *Tbx4*-mutant hindlimb buds, *dHand* is expressed along the entire distal margin of the bud, indicating a defect in anterior/posterior patterning (Fig. 6G,H). *dHand* is normally excluded from the anterior limb bud by *Gli3* expression in the anterior, which is normal in *Tbx4* mutants (data not shown). *Tbx3*, which is also required for posterior limb formation (Bamshad et al., 1997; Davenport et al., 2003), is correctly expressed in the posterior margin of *Tbx4*-mutant hindlimb buds (Fig. 6I,J).

Tbx2 is also normally expressed in the posterior hindlimb margin at this stage, although no function in limb development has yet been assigned to it. *Tbx2* is absent from *Tbx4*-mutant hindlimb buds (Fig. 6K,L). This demonstrates that *Tbx4* lies upstream of *Tbx2* in at least two tissues, the allantois and the hindlimb.

DISCUSSION

Function of the *Tbx4*-mutant alleles

Our work describes two mutant alleles of the *Tbx4* gene that are phenotypically indistinguishable. The *Tbx4^{tm1.1Pa}* allele excises exon 5, which encodes most of the 5' half of the T-box domain of *Tbx4*. Because exon 5 is a non-unit exon, this excision also creates a frameshift in subsequent exons. The *Tbx4^{tm1.1Pa}* transcript, if translated, would produce only the N-terminal 138 amino acids of the protein. This hypothetical truncated protein would lack both the DNA-binding T-box domain and the large C-terminal domain, and is therefore predicted to be a functional null.

The *Tbx4^{tm1.1Pa}* allele consists of the insertion of a lox site and a floxed selection cassette into the introns surrounding exon 5, which creates no disruption of the *Tbx4* exon sequences or splice sites. Nevertheless, the phenotype of this allele is indistinguishable from the null, which indicates that these intronic insertions result in profound gene disruption. This disruption is presumably due to the exogenous promoter and cryptic splice sites found in the *neo* selection cassette, both of which have been shown to disrupt gene function when inserted into non-coding regions (McDevitt et al., 1997; Meyers et al., 1998; Nagy et al., 1998). These reports have shown only partial gene disruption; however, they involve only the *neo* cassette,

whereas we have used a *neo-tk* cassette. The addition of the *tk* gene results in an additional exogenous promoter and a polyadenylation site, which probably exacerbates interference by the *neo-tk* cassette. Alternatively, the *Tbx4* locus could be especially susceptible to splicing disruption, or *Tbx4* dosage sensitivity could be such that even partial disruption of *Tbx4* passes below a minimum threshold limit.

Allantois development in *Tbx4* mutants

Tbx4 mutants first exhibit a defect at 8.0 dpc, when they demonstrate a short allantois and failure of chorioallantoic fusion. At this age, homozygous-mutant, heterozygous and wild-type embryos display considerable overlap in phenotype (Fig. 3A). This stage marks the only appearance of a heterozygous effect of *Tbx4*, resulting in a delay in chorioallantoic fusion, although all heterozygous embryos eventually undergo chorioallantoic fusion and become indistinguishable from their wild-type littermates. However, homozygous-*Tbx4* mutants are readily distinguished from littermates by the failure of chorioallantoic fusion.

We have attributed the death of *Tbx4*-homozygous mutants at 10.5 dpc to failure of chorioallantoic fusion. In the absence of an umbilicus, the embryo cannot exchange gasses, nutrients or waste with the maternal blood supply. Absence of the umbilicus also alters normal blood flow patterns, most probably accounting for the observed hemorrhage and pericardial edema. Several other mutations that result in failure of chorioallantoic fusion produce similar phenotypes (Gurtner et al., 1995; Kwee et al., 1995; Tremblay et al., 2001; Yang et al., 1995).

Extension of the allantois from the posterior axis of the embryo to the chorion results from a number of processes, including influx of cells from the primitive streak, cellular proliferation and cavitation of distal tissue (Downs and Bertler, 2000). Embryos mutant for *Tbx4* have a normal primitive streak, as evidenced by normal expression of *T*, and proliferation in the allantois is also normal (Fig. 2B,C). However, cells near the tip of the *Tbx4*-mutant allantois undergo apoptosis (Fig. 2D,E). Factors required for cell survival in the allantois are not known. However, it is interesting to note that *Tbx2* is downregulated in *Tbx4*-mutant allantoises, and previous work has implied a requirement for *Tbx2* to prevent cell cycle arrest in rapidly proliferating tissues (Jacobs et al., 2000). Therefore, the role of *Tbx4* in the allantois may be the maintenance of *Tbx2*-mediated suppression of apoptosis.

Also, in contrast to normal development, the allantois in *Tbx4*-mutant embryos shows no cavitation near the distal tip. Although the molecular nature of this defect is unknown, we find it relevant that T-box genes have been implicated in the regulation of adhesion molecules in several systems. In zebrafish and *Xenopus*, T-box genes have been shown to regulate paraxial protocadherin (Kim et al., 1998; Yamamoto et al., 1998), and, in mice, *Tbr1* is a direct activator of *reelin*, an extracellular matrix glycoprotein. Mouse mutations in *T* produce primitive streak cells with a substrate-dependent migration defect (Hashimoto et al., 1987), and work with *Fgfr1*-mutant mice has revealed links between *T* and cadherin regulation (Ciruna and Rossant, 2001). This data suggests that the failure of allantois cavitation could be caused by misregulation of adhesion genes in *Tbx4* mutants.

Despite the various defects inhibiting allantois growth, as many as 15% of *Tbx4*-mutant allantoises observed had extended into the dome of the chorion at the 4- to 5-somite stage (Fig. 1A; L.A.N. and V.E.P., unpublished). However, chorioallantoic fusion rarely occurs in *Tbx4* mutants. Of more than 250 mutant embryos observed, only two had established any connection between the allantois and chorion. The lack of expression of *Vcam1*, a key adhesion molecule affecting this process (Gurtner et al., 1995; Kwee et al., 1995), in the *Tbx4* mutants is clearly a contributing factor. However, *Vcam1* homozygous-null embryos undergo chorioallantoic fusion in 20-50% of cases, so this defect alone is insufficient to explain the *Tbx4* phenotype. It is possible that the combination of the lack of VCAM1 protein and the extensive apoptosis in the tip of the allantois produces a synergistic loss of chorioallantoic fusion potential.

In addition to the failure of chorioallantoic fusion in *Tbx4* mutants, there is also a block in vascular remodeling in the allantois. Endothelial cells, evidenced by positive staining for PECAM, successfully differentiate from allantoic mesenchyme, but they remain as discreet clumps of cells and fail to remodel into primary vessels. These clumps presumably correspond to the double-layered vesicles seen histologically, and are also presumably the progenitors of the blood-filled vesicles seen morphologically in the residual allantois at 10.5 dpc. It is unclear whether the failure of endothelial cells to coalesce into vessels in *Tbx4* mutants is cell autonomous, or represents a defect in signaling or adhesion characteristics in surrounding cells of the allantois.

Bmp4 has previously been identified as a key regulator of allantois development. It is required in the extra-embryonic ectoderm for allantois induction, and later in the allantois itself for normal development and chorioallantoic fusion. The phenotype produced by the absence of *Bmp4* in the allantois shares many points of similarity with the *Tbx4* phenotype. Both exhibit a shortened, unfused allantois with no apparent proliferative defect, neither express VCAM1 at the tip of the allantois and both have defects in the vascularization of the allantois. Previous work has suggested that T-box genes can be regulated by BMP signaling (Koshiba-Takeuchi et al., 2000; Smith et al., 1991; Yamada et al., 2000), and the observation that *Bmp4* expression in the allantois is unaffected by the loss of *Tbx4* is consistent with an upstream role for *Bmp4* with respect to *Tbx4*. However, the absence of *Bmp4* also severely disrupts PGC placement and formation, whereas this process is unaffected by a lack of *Tbx4*. It may be that *Tbx4* is a downstream effector of *Bmp4* in the allantois, whereas other molecules act as intermediaries for *Bmp4* signaling to the PGCs.

A model for *Tbx4* function in the hindlimb

Much is known about the initiation of limb morphogenesis (Tickle and Munsterberg, 2001). Anterior/posterior, dorsal/ventral and distal/proximal axes are all set up early in limb bud formation. *Fgf10* signaling from the limb mesenchyme induces an apical ectodermal ridge (AER) in the overlying ectoderm. The AER, in turn, signals back to the mesenchyme through *Fgf8* and *Fgf4* to maintain *Fgf10* in the region underlying the AER known as the progress zone. *Fgf10* is required to maintain proliferation in the progress zone, which drives limb outgrowth. This represents an FGF-mediated positive feedback

loop, which is required for limb development. A second feedback loop is set up between the AER and a region in the posterior mesenchyme known as the zone of polarizing activity (ZPA). The ZPA directs posterior patterning in the limb and is marked chiefly by the expression of the secreted signaling molecule *Shh*. Failure of either of these feedback loops results in the absence or dramatic reduction of limb growth and patterning.

At early 10.5 dpc, *Tbx4*-mutant embryos have morphologically obvious hindlimb buds that are similar to stage-matched wild-type controls. In many respects, the initiation of these hindlimb buds is normal. Hindlimb specificity in *Tbx4* mutants appears unaltered, as indicated by the presence of *Ptx1* and *Tbx4* expression, and the lack of *Tbx5* expression. Ventrally restricted expression of *Msx2* and correct positioning of *Fgf8* expression both suggest that dorsoventral patterning is unaffected by the absence of *Tbx4* (Pizette et al., 2001). Several genes known to be involved in limb outgrowth and/or FGF reciprocal signaling are correctly activated, including *Msx1* and the gene encoding dp-ERK in the progress zone, *Fgf8* in the presumptive AER and *Twist* throughout the hindlimb mesenchyme.

However, the ablation of *Tbx4* does result in some defects in anterior/posterior patterning of the hindlimb. In normal limbs, *dHand* is restricted to the posterior limb bud by the action of *Gli3* in the anterior limb bud (te Welscher et al., 2002). *dHand* induces *Shh* in the posterior limb bud, and *Shh* signaling is key for the activity of the ZPA. *Tbx4*-mutant embryos die prior to the expression of *Shh*, but, in mutant embryos, *dHand* is shifted from posterior-specific expression to expression throughout the mutant hindlimb bud despite normal expression of *Gli3*. Conversely, *Tbx3*, which is known to affect posterior limb development in mouse and human (Bamshad et al., 1997; Davenport et al., 2003), is correctly expressed in the posterior margin of the *Tbx4*-mutant hindlimb. *Tbx2*, which is also normally expressed in the posterior margin of the hindlimb bud, is absent in *Tbx4*-mutant hindlimbs. As no function has been identified for *Tbx2* in limb development, this is notable chiefly because it shows that *Tbx2* expression is ablated in *Tbx4* mutants in both of the tissues where the two genes are co-expressed prior to the death of the mutant embryos, thus revealing a role for a T-box gene in regulating another T-box gene.

Despite successful induction of the hindlimb bud, and of many outgrowth and patterning genes therein, neither hindlimb outgrowth nor *Fgf10* expression is maintained in *Tbx4*-mutant hindlimbs. Initial FGF signaling is apparently normal in *Tbx4*-mutant hindlimbs, as visualized by the induction of *Fgf8* in the ectoderm and phosphorylation of ERK in the mesenchyme. However, by 10.5 dpc, *Fgf10* is absent from the distal mutant hindlimb buds and only residual flank expression can be seen. As the absence of *Fgf10* has been shown to ablate limb formation (Min et al., 1998; Sekine et al., 1999), it is unsurprising that *Tbx4*-mutant hindlimbs fail to progress when grown in culture.

Similar roles of *Tbx4* in the forelimb and *Tbx5* in the hindlimb have been proposed in previous studies (Gibson-Brown et al., 1998; Logan and Tabin, 1999; Ohuchi et al., 1998; Rodriguez-Esteban et al., 1999; Ruvinsky and Gibson-Brown, 2000; Saito et al., 2002; Tanaka et al., 2002). This study, and the recently published study of *Tbx5* in the forelimb

(Agarwal et al., 2003), reveals that the roles of *Tbx4* and *Tbx5* are subtly different. In each case, the specification of the relevant limb field proceeds despite the lack of *Tbx4* or *Tbx5*. However, in the case of *Tbx4* ablation, FGF signaling is initiated but not maintained, whereas *Tbx5* ablation precludes any expression of *Fgf10* or *Fgf8*.

By marker analysis, the *Tbx4* mutation closely resembles genetic manipulations that disrupt reciprocal FGF signaling from the AER to the limb mesenchyme, such as mutations in *Twist*, an upstream regulator of *Fgfr1* in limb mesenchyme (O'Rourke et al., 2002; Zuniga et al., 2002), and the AER-specific ablation of both *Fgf8* and *Fgf4* (Sun et al., 2002). All of these disruptions exhibit successful induction of AER-specific FGFs, disruption of some but not all anterior/posterior axis markers, normal induction of FGF-independent limb markers, such as *Msx1*, and rapid downregulation of *Fgf10*. In particular, mutations in *Twist* result in the expansion of *Shh* and *Hoxd11* into the anterior of the limb bud, whereas in the absence of *Fgf8* and *Fgf4*, the anterior expression of *Alx4* is expanded posteriorly. The anterior expansion of *Shh* and *Hoxd11* occurs despite the normal expression of *Gli3* in the anterior of these limbs, demonstrating the importance of FGF signaling in the *Gli3*-dependent maintenance of the anterior/posterior axis of the limb bud.

Our data shows that FGF reciprocal signaling in *Tbx4*-

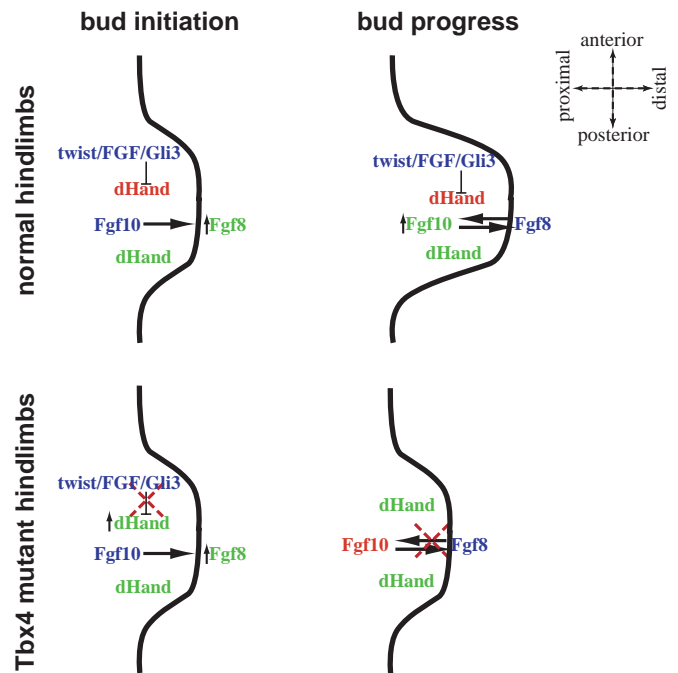


Fig. 7. A proposed model for *Tbx4* function in the hindlimb. During hindlimb initiation in normal embryos, *dHand* is repressed in the anterior but not the posterior limb bud by the FGF-dependent action of *Gli3*. Simultaneously, *Fgf10* signals to the overlying ectoderm to upregulate *Fgf8*. As the limb bud progresses, *dHand* repression in the anterior limb bud is maintained, while *Fgf8* reciprocal signaling maintains *Fgf10* in the limb mesenchyme. In the mutant hindlimb bud, failure of *Tbx4*-mediated FGF signaling leads to derepression of *dHand* in the anterior limb bud. Mesenchymal FGF signaling to the ectoderm is normal and *Fgf8* is properly upregulated, but reciprocal signaling fails and *Fgf10* is not maintained.

mutant hindlimb mesenchyme is successful up to the point of ERK phosphorylation by the FGF-activated MAPK cascade. However, we observed a failure in the maintenance of *Fgf10* and an expansion of the posterior limb domain, as evidenced by *dHand* expression, both of which are consistent with a failure in FGF signaling. This suggests that the role of *Tbx4* in early limb development is to transduce the signal of the MAPK cascade to its final limb targets (Fig. 7), including both anterior *dHand* repression and *Fgf10* upregulation. Aside from *Gli3*, the transcriptional co-factors involved in *dHand* repression are not known, but it is possible that *Tbx4* is an FGF-sensitive, direct repressor of this gene; alternatively, the derepression of *dHand* in *Tbx4*-mutant hindlimbs could be a secondary result of disrupted FGF signaling. *Fgf10* is probably a direct target of *Tbx4*, as T-box binding sites have been observed in the *Fgf10* promoter and *Fgf10* is capable of T-box dependent reporter gene activation in vitro (Agarwal et al., 2003; Ng et al., 2002). It seems likely therefore that *Tbx4* is a MAPK-sensitive, direct regulator of both *dHand* and *Fgf10*.

We thank members of the laboratory, especially Kat Hadjantonakis and Sarah Goldin for helpful discussions, G. Shackelford, A. Joyner, A. McMahon, and G. Martin for generously supplying probes, and Peter Mombaerts for the floxed PGK-*neo* PGK-*thymidine kinase* double selection cassette. This work was supported by a grant from the NIH (HD33082) (to V.E.P.) and a National Science Foundation pre-doctoral fellowship (to L.A.N.).

REFERENCES

- Agarwal, P., Wylie, J. N., Galceran, J., Arkhitko, O., Li, C., Deng, C., Grosschedl, R. and Bruneau, B. G. (2003). Tbx5 is essential for forelimb bud initiation following patterning of the limb field in the mouse embryo. *Development* **130**, 623-633.
- Agulnik, S. I., Garvey, N., Hancock, S., Ruvinsky, I., Chapman, D. L., Agulnik, I., Bollag, R., Papaioannou, V. and Silver, L. M. (1996). Evolution of mouse T-box genes by tandem duplication and cluster dispersion. *Genetics* **144**, 249-254.
- Bamshad, M., Lin, R. C., Law, D. J., Watkins, W. S., Krakowiak, P. A., Moore, M. E., Franceschini, P., Lala, R., Holmes, L. B., Gebuhr, T. C. et al. (1997). Mutations in human TBX3 alter limb, apocrine and genital development in ulnar-mammary syndrome. *Nat. Genet.* **16**, 311-315.
- Basson, C. T., Bachinsky, D. R., Lin, R. C., Levi, T., Elkins, J. A., Soultis, J., Grayzel, D., Kroupouzou, E., Traill, T. A., Leblanc-Straccesi, J. et al. (1997). Mutations in human TBX5 [corrected] cause limb and cardiac malformation in Holt-Oram syndrome. *Nat. Genet.* **15**, 30-35.
- Bruneau, B. G., Nemer, G., Schmitt, J. P., Charron, F., Robitaille, L., Caron, S., Conner, D. A., Gessler, M., Nemer, M., Seidman, C. E. et al. (2001). A murine model of Holt-Oram syndrome defines roles of the T-box transcription factor Tbx5 in cardiogenesis and disease. *Cell* **106**, 709-721.
- Chang, H., Huylebroeck, D., Verschuere, K., Guo, Q., Matzuk, M. M. and Zwijsen, A. (1999). Smad5 knockout mice die at mid-gestation due to multiple embryonic and extraembryonic defects. *Development* **126**, 1631-1642.
- Chapman, D. L., Garvey, N., Hancock, S., Alexiou, M., Agulnik, S. I., Gibson-Brown, J. J., Cebra-Thomas, J., Bollag, R. J., Silver, L. M. and Papaioannou, V. E. (1996). Expression of the T-box family genes, Tbx1-Tbx5, during early mouse development. *Dev. Dyn.* **206**, 379-390.
- Ciruna, B. and Rossant, J. (2001). FGF signaling regulates mesoderm cell fate specification and morphogenetic movement at the primitive streak. *Dev. Cell* **1**, 37-49.
- Davenport, T. G., Jerome-Majewska, L. A. and Papaioannou, V. E. (2003). Mammary gland, limb and yolk sac defects in mice lacking Tbx3, the gene mutated in human ulnar-mammary syndrome. *Development* **130**, 2263-2273.
- Davis, C. A. (1993). Whole-mount immunohistochemistry. *Methods Enzymol.* **225**, 502-516.
- Downs, K. M. and Bertler, C. (2000). Growth in the pre-fusion murine allantois. *Anat. Embryol.* **202**, 323-331.
- Fujiwara, T., Dunn, N. R. and Hogan, B. L. M. (2001). Bone morphogenetic protein 4 in the extraembryonic mesoderm is required for allantois development and the localization and survival of primordial germ cells in the mouse. *Proc. Natl. Acad. Sci. USA* **98**, 13739-13744.
- Gibson-Brown, J. J., Agulnik, S. I., Chapman, D. L., Alexiou, M., Garvey, N., Silver, L. M. and Papaioannou, V. E. (1996). Evidence of a role for T-box genes in the evolution of limb morphogenesis and the specification of forelimb/hindlimb identity. *Mech. Dev.* **56**, 93-101.
- Gibson-Brown, J. J., Agulnik, S. I., Silver, L. M., Niswander, L. and Papaioannou, V. E. (1998). Involvement of T-box genes Tbx2-Tbx5 in vertebrate limb specification and development. *Development* **125**, 2499-2509.
- Gurtner, G. C., Davis, V., Li, H., McCoy, M. J., Sharpe, A. and Cybulsky, M. I. (1995). Targeted disruption of the murine VCAM1 gene: essential role of VCAM-1 in chorioallantoic fusion and placentation. *Genes Dev.* **9**, 1-14.
- Hashimoto, K., Fujimoto, H. and Nakatsuji, N. (1987). An ECM substratum allows mouse mesodermal cells isolated from the primitive streak to exhibit motility similar to that inside the embryo and reveals a deficiency in the T/T mutant cells. *Development* **100**, 587-598.
- Isaac, A., Rodriguez-Esteban, C., Ryan, A., Altabef, M., Tsukui, T., Patel, K., Tickle, C. and Izpisua-Belmonte, J. C. (1998). Tbx genes and limb identity in chick embryo development. *Development* **125**, 1867-1875.
- Jacobs, J. J., Keblusek, P., Robanus-Maandag, E., Kristel, P., Lingbeek, M., Nederlof, P. M., van Welsem, T., van de Vijver, M. J., Koh, E. Y., Daley, G. Q. et al. (2000). Senescence bypass screen identifies TBX2, which represses Cdkn2a (p19(ARF)) and is amplified in a subset of human breast cancers. *Nat. Genet.* **26**, 291-299.
- Kim, S. H., Yamamoto, A., Bouwmeester, T., Agius, E. and Robertis, E. M. (1998). The role of paraxial protocadherin in selective adhesion and cell movements of the mesoderm during *Xenopus* gastrulation. *Development* **125**, 4681-4690.
- Koshiba-Takeuchi, K., Takeuchi, J. K., Matsumoto, K., Momose, T., Uno, K., Hoepker, V., Ogura, K., Takahashi, N., Nakamura, H., Yasuda, K. et al. (2000). Tbx5 and the retinotectum projection. *Science* **287**, 134-137.
- Kwee, L., Baldwin, H. S., Shen, H. M., Stewart, C. L., Buck, C., Buck, C. A. and Labow, M. A. (1995). Defective development of the embryonic and extraembryonic circulatory systems in vascular cell adhesion molecule (VCAM-1) deficient mice. *Development* **121**, 489-503.
- Lanctot, C., Lamolet, B. and Drouin, J. (1997). The bicoid-related homeoprotein Ptx1 defines the most anterior domain of the embryo and differentiates posterior from anterior lateral mesoderm. *Development* **124**, 2807-2817.
- Lanctot, C., Moreau, A., Chamberland, M., Tremblay, M. L. and Drouin, J. (1999). Hindlimb patterning and mandible development require the Ptx1 gene. *Development* **126**, 1805-1810.
- Lawson, K. A., Dunn, N. R., Roelen, B. A., Zeinstra, L. M., Davis, A. M., Wright, C. V., Korving, J. P. and Hogan, B. L. (1999). Bmp4 is required for the generation of primordial germ cells in the mouse embryo. *Genes Dev.* **13**, 424-436.
- Lechleider, R. J., Ryan, J. L., Garrett, L., Eng, C., Deng, C., Wynshaw-Boris, A. and Roberts, A. B. (2001). Targeted mutagenesis of Smad1 reveals an essential role in chorioallantoic fusion. *Dev. Biol.* **240**, 157-167.
- Lewandoski, M. and Martin, G. R. (1997). Cre-mediated chromosome loss in mice. *Nat. Genet.* **17**, 223-225.
- Li, Q. Y., Newbury-Ecob, R. A., Terrett, J. A., Wilson, D. I., Curtis, A. R., Yi, C. H., Gebuhr, T., Bullen, P. J., Robson, S. C., Strachan, T. et al. (1997). Holt-Oram syndrome is caused by mutations in TBX5, a member of the Brachyury (T) gene family. *Nat. Genet.* **15**, 21-29.
- Logan, M. and Tabin, C. J. (1999). Role of Pitx1 upstream of Tbx4 in specification of hindlimb identity. *Science* **283**, 1736-1739.
- Mahlapuu, M., Ormestad, M., Enerback, S. and Carlsson, P. (2001). The forkhead transcription factor Foxf1 is required for differentiation of extraembryonic and lateral plate mesoderm. *Development* **128**, 155-166.
- Martin, G. (2001). Making a vertebrate limb: new players enter from the wings. *BioEssays* **23**, 865-868.
- Maxwell, F., Maxwell, I. H. and Glode, L. M. (1987). Cloning, sequence determination, and expression in transfected cells of the coding sequence for the tox 176 attenuated diphtheria toxin A chain. *Mol. Cell. Biol.* **7**, 1576-1579.
- McDevitt, M. A., Shivdasani, R. A., Fujiwara, Y., Yang, H. and Orkin, S. H. (1997). A "knockdown" mutation created by cis-element gene targeting

- reveals the dependence of erythroid cell maturation on the level of transcription factor GATA-1. *Proc. Natl. Acad. Sci. USA* **94**, 6781-6785.
- Meyers, E. N., Lewandoski, M. and Martin, G. R.** (1998). An Fgf8 mutant allelic series generated by Cre- and Flp-mediated recombination. *Nat. Genet.* **18**, 136-141.
- Min, H., Danilenko, D. M., Scully, S. A., Bolon, B., Ring, B. D., Tarpley, J. E., DeRose, M. and Simonet, W. S.** (1998). Fgf-10 is required for both limb and lung development and exhibits striking functional similarity to Drosophila branchless. *Genes Dev.* **12**, 3156-3161.
- Nagy, A., Rossant, J., Nagy, R., Abramow-Newerly, W. and Roder, J. C.** (1993). Derivation of completely cell culture-derived mice from early-passage embryonic stem cells. *Proc. Natl. Acad. Sci. USA* **90**, 8424-8428.
- Nagy, A., Moens, C., Ivanyi, E., Pawling, J., Gertsenstein, M., Hadjantonakis, A. K., Purity, M. and Rossant, J.** (1998). Dissecting the role of N-myc in development using a single targeting vector to generate a series of alleles. *Curr. Biol.* **8**, 661-664.
- Ng, J. K., Kawakami, Y., Buscher, D., Raya, A., Itoh, T., Koth, C. M., Rodriguez Esteban, C., Rodriguez-Leon, J., Garrity, D. M., Fishman, M. C. et al.** (2002). The limb identity gene Tbx5 promotes limb initiation by interacting with Wnt2b and Fgf10. *Development* **129**, 5161-5170.
- O'Rourke, M. P., Soo, K., Behringer, R. R., Hui, C. C. and Tam, P. P.** (2002). Twist plays an essential role in FGF and SHH signal transduction during mouse limb development. *Dev. Biol.* **248**, 143-156.
- Ohuchi, H., Takeuchi, J., Yoshioka, H., Ishimaru, Y., Ogura, K., Takahashi, N., Ogura, T. and Noji, S.** (1998). Correlation of wing-leg identity in ectopic FGF-induced chimeric limbs with the differential expression of chick Tbx5 and Tbx4. *Development* **125**, 51-60.
- Oka, C., Nakano, T., Wakeham, A., de la Pompa, J. L., Mori, C., Sakai, T., Okazaki, S., Kawauchi, M., Shiota, K., Mak, T. M. et al.** (1995). Disruption of the mouse RBP-J kappa gene results in early embryonic death. *Development* **121**, 3291-3301.
- Papaioannou, V. E.** (2001). T-box genes in development: From hydra to humans. *Int. Rev. Cytol.* **207**, 1-70.
- Pizette, S., Abate-Shen, C. and Niswander, L.** (2001). BMP controls proximodistal outgrowth, via induction of the apical ectodermal ridge, and dorsoventral patterning in the vertebrate limb. *Development* **128**, 4463-4474.
- Rodriguez-Esteban, C., Tsukui, T., Yonei, S., Magallon, J., Tamura, K. and Izpisua Belmonte, J. C.** (1999). The T-box genes Tbx4 and Tbx5 regulate limb outgrowth and identity. *Nature* **398**, 814-818.
- Ruvinsky, I. and Gibson-Brown, J. J.** (2000). Genetic and developmental bases of serial homology in vertebrate limb evolution. *Development* **127**, 5233-5244.
- Ruvinsky, I., Silver, L. M. and Gibson-Brown, J. J.** (2000). Phylogenetic analysis of T-Box genes demonstrates the importance of amphioxus for understanding evolution of the vertebrate genome. *Genetics* **156**, 1249-1257.
- Saito, D., Yonei-Tamura, S., Kano, K., Ide, H. and Tamura, K.** (2002). Specification and determination of limb identity: evidence for inhibitory regulation of Tbx gene expression. *Development* **129**, 211-220.
- Sekine, K., Ohuchi, H., Fujiwara, M., Yamasaki, M., Yoshizawa, T., Sato, T., Yagishita, N., Matsui, D., Koga, Y., Itoh, N. et al.** (1999). Fgf10 is essential for limb and lung formation. *Nat. Genet.* **21**, 138-141.
- Shang, J., Luo, Y. and Clayton, D. A.** (1997). Backfoot is a novel homeobox gene expressed in the mesenchyme of developing hind limb. *Dev. Dyn.* **209**, 242-253.
- Smith, J. C., Price, B. M. J., Green, J. B. A., Weigel, D. and Herrmann, B. G.** (1991). Expression of a Xenopus homolog of Brachyury (T) is an immediate-early response to mesoderm induction. *Cell* **67**, 79-87.
- Solloway, M. J. and Robertson, E. J.** (1999). Early embryonic lethality in Bmp5;Bmp7 double mutant mice suggests functional redundancy within the 60A subgroup. *Development* **126**, 1753-1768.
- Sun, X., Mariani, F. V. and Martin, G. R.** (2002). Functions of FGF signalling from the apical ectodermal ridge in limb development. *Nature* **418**, 501-508.
- Szeto, D. P., Rodriguez-Esteban, C., Ryan, A. K., O'Connell, S. M., Liu, F., Kioussi, C., Gleiberman, A. S., Izpisua-Belmonte, J. C. and Rosenfeld, M. G.** (1999). Role of the Bicoid-related homeodomain factor Pitx1 in specifying hindlimb morphogenesis and pituitary development. *Genes Dev.* **13**, 484-494.
- Takeuchi, J. K., Koshiba-Takeuchi, K., Matsumoto, K., Vogel-Hopker, A., Naitoh-Matsuo, M., Ogura, K., Takahashi, N., Yasuda, K. and Ogura, T.** (1999). Tbx5 and Tbx4 genes determine the wing/leg identity of limb buds. *Nature* **398**, 810-814.
- Tanaka, M., Munsterberg, A., Anderson, W. G., Prescott, A. R., Hazon, N. and Tickle, C.** (2002). Fin development in a cartilaginous fish and the origin of vertebrate limbs. *Nature* **416**, 527-531.
- te Welscher, P., Fernandez-Teran, M., Ros, M. A. and Zeller, R.** (2002). Mutual genetic antagonism involving GLI3 and dHAND prepatterns the vertebrate limb bud mesenchyme prior to SHH signaling. *Genes Dev.* **16**, 421-426.
- Tickle, C. and Munsterberg, A.** (2001). Vertebrate limb development – the early stages in chick and mouse. *Curr. Opin. Genet. Dev.* **11**, 476-481.
- Tremblay, K. D., Dunn, N. R. and Robertson, E. J.** (2001). Mouse embryos lacking Smad1 signals display defects in extra-embryonic tissues and germ cell formation. *Development* **128**, 3609-3621.
- Wang, Y. and Sassoon, D.** (1995). Ectoderm-mesenchyme and mesenchyme-mesenchyme interactions regulate Msx-1 expression and cellular differentiation in the murine limb bud. *Dev. Biol.* **168**, 374-382.
- Wilkinson, D. G. and Nieto, M. A.** (1993). Detection of messenger RNA by in situ hybridization to tissue sections and whole mounts. *Methods Enzymol.* **225**, 361-373.
- Yamada, M., Revelli, J. P., Eichele, G., Barron, M. and Schwartz, R. J.** (2000). Expression of chick Tbx-2, Tbx-3, and Tbx-5 genes during early heart development: Evidence for BMP2 induction of Tbx2. *Dev. Biol.* **228**, 95-105.
- Yamamoto, A., Amacher, S. L., Kim, S. H., Geissert, D., Kimmel, C. B. and De Robertis, E. M.** (1998). Zebrafish paraxial protocadherin is a downstream target of spadetail involved in morphogenesis of gastrula mesoderm. *Development* **125**, 3389-3397.
- Yang, J. T., Rayburn, H. and Hynes, R. O.** (1995). Cell adhesion events mediated by alpha 4 integrins are essential in placental and cardiac development. *Development* **121**, 549-560.
- Ying, Y., Liu, X. M., Marble, A., Lawson, K. A. and Zhao, G. Q.** (2000). Requirement of Bmp8b for the generation of primordial germ cells in the mouse. *Mol. Endocrinol.* **14**, 1053-1063.
- Zuniga, A., Quillet, R., Perrin-Schmitt, F. and Zeller, R.** (2002). Mouse Twist is required for fibroblast growth factor-mediated epithelial-mesenchymal signalling and cell survival during limb morphogenesis. *Mech. Dev.* **114**, 51-59.